PORTLAND PRESS

Research Article

Identification of novel genes associated with a poor prognosis in pancreatic ductal adenocarcinoma via a bioinformatics analysis

Jun Zhou[1], Xiaoliang Hui[1], Ying Mao[1] and ⓘ Liya Fan[2]

[1]Department of General Ward 1, Zhejiang Hospital of Lingyin District, Zhejiang, China; [2]Department of Gastroenterology, Zhejiang Hospital of Sandun District, Zhejiang, China

Correspondence: Liya Fan (2059722762@qq.com)

OPEN ACCESS

Pancreatic ductal adenocarcinoma (PDAC) is a class of the commonest malignant carcinomas. The present study aimed to elucidate the potential biomarker and prognostic targets in PDAC. The array data of GSE41368, GSE43795, GSE55643, and GSE41369 were downloaded from Gene Expression Omnibus (GEO) database. The differentially expressed genes (DEGs) and differentially expressed microRNAs (DEmiRNAs) in PDAC were obtained by using GEO2R, and overlapped DEGs were acquired with Venn Diagrams. Functional enrichment analysis of overlapped DEGs and DEmiRNAs was conducted with Metascape and FunRich, respectively. The protein–protein interaction (PPI) network of overlapped DEGs was constructed by STRING and visualized with Cytoscape. Overall survival (OS) of DEmiRNAs and hub genes were investigated by Kaplan–Meier (KM) plotter (KM plotter). Transcriptional data and correlation analyses among hub genes were verified through GEPIA and Human Protein Atlas (HPA). Additionally, miRNA targets were searched using miRTarBase, then miRNA–DEG regulatory network was visualized with Cytoscape. A total of 32 DEmiRNAs and 150 overlapped DEGs were identified, and Metascape showed that DEGs were significantly enriched in cellular chemical homeostasis and pathways in cancer, while DEmiRNAs were mainly enriched in signal transduction and Glypican pathway. Moreover, seven hub genes with a high degree, namely, V-myc avian myelocytomatosis viral oncogene homolog (MYC), solute carrier family 2 member 1 (SLC2A1), PKM, plasminogen activator, urokinase (PLAU), peroxisome proliferator activated receptor γ (PPARG), MET proto-oncogene, receptor tyrosine kinase (MET), and integrin subunit α 3 (ITGA3), were identified and found to be up-regulated between PDAC and normal tissues. miR-135b, miR-221, miR-21, miR-27a, miR-199b-5p, miR-143, miR-196a, miR-655, miR-455-3p, miR-744 and hub genes predicted poor OS of PDAC. An integrative bioinformatics analysis identified several hub genes that may serve as potential biomarkers or targets for early diagnosis and precision target treatment of PDAC.

Introduction

Pancreatic ductal adenocarcinoma (PDAC) is the most common pancreatic neoplasm, accounting for approximately 90% of all pancreatic cancers (PCs), with a poor overall survival (OS) rate of 5–8% [1,2]. Over 52% of cases are diagnosed in a distal metastasis stage, with only 3% showing a 5-year OS benefit [3]. Currently, surgical extirpation is the primary curative strategy; however, most patients with PDAC do not display any specific early signs of clinical disease, which causes missed opportunities for surgery due to the progression of cancer without detection. The preferred and most promising strategy for PC treatment is surgical resection, and the detection of PC during the surgically resectable stages has vast importance for ameliorating the survival benefit of patients with PC [4]. Therefore, an exact, early diagnosis of PDAC

is needed, and the discovery of molecular biomarkers and targets could be another promising strategy to promote further developments in therapeutic modalities and strategies.

Various factors are associated with the growth and development of cancer and PDAC, including mutation, age, sex, ethnicity, cigarette smoking, and viral and bacterial infections [5–9]. The association of infectious agents in the etiology of different types of cancer has piqued the interest of scientists in recent years. Recent data have shown the involvement of *Mycoplasma hominis*, *Chlamydia pneumoniae*, and *Escherichia coli* infection in the etiology of prostate cancer, lung cancer, and colon cancer, respectively [9–12]. Recently, a wealth of previous studies have reported that microRNAs (miRNAs), a class of noncoding RNAs characterized by approximately 22 nucleotides in length, can inhibit the stability and translation of messenger RNAs (mRNAs) through binding to the specific sequence of genes, which are used as potential biomarkers for different kinds of cancer. Su et al. (2018) [13] employed Weighted Gene Co-Expression Network Analysis (WGCNA) to analyze 88 patients with PDAC and 19 healthy controls and reported that five miRNAs (miR-3201, miR-890, miR-16-2-3p, miR-877, and miR-602) were defined as promising diagnostic and prognostic biomarkers for PDAC. Additionally, miR-661 is up-regulated in PDAC and simultaneously promotes the protein expression level of transcription factor 4, β-catenin, and cyclin D1, which are associated with the Wnt signaling pathway *in vitro*, and can be used as a prognostic marker in suspicious pancreatic lesions [14]. Wei et al. (2018) [15] demonstrated that the overexpression of miR-23b-3p decreased tumor volume or even prevented the formation of tumors by directly down-regulating annexin A2 (ANXA2). Many biomarkers and therapeutic targets play a vital role in the diagnosis and treatment of PDAC. However, no breakthrough in the conventional treatment strategy has been investigated because of the difficulty in the early diagnosis and ominous prognosis of PDAC, and there is urgent need to identify more genetic information about pivotal genes in the progression of this disease.

Several *in silico* bioinformatics tools are widely applied to assess gene expression levels, to screen unique genes from RNA-sequencing and next-generation sequencing data, and to explore their possible implication in the growth of different types of cancer [16–18]. Currently, microarrays have been widely employed to detect genetic alterations during the initiation and progression of tumorigenesis. Accumulating data on malignancy are available at the authoritative Gene Expression Omnibus (GEO) (http://www.ncbi.nlm.nih.gov/geo/) genomics data repository that includes microarray and high-throughput sequencing data [19]. In the present paper, we employed mRNA microarray data of GSE41368 [20], GSE43795 [21], and GSE55643 [22] and miRNA microarray data of GSE41369 [20] to identify the differentially expressed genes (DEGs) and differentially expressed miRNAs (DEmiRNAs) and to explore the potential therapeutic targets as well as the prognostic value of PDAC. Compared with a single expression profile, the bioinformatics analysis of the overlapping DEGs in more chips could be more reliable. In the current study, we performed a comprehensive bioinformatics analysis to identify hub overlapping DEGs, and GO terms and KEGG pathway enrichment analyses of the DEGs and DEmiRNAs were performed. A protein–protein interaction (PPI) network and a DEmiRNA target network were constructed to assess the interactions between the DEmiRNAs and hub genes. Moreover, seven significant hub genes and ten DEmiRNAs were revealed to be associated with OS in PDAC by the Kaplan–Meier (KM) plotter (KM plotter). In addition, the mRNA expression level, correlation analysis and protein expression of the hub genes were validated with the GEPIA and Human Protein Atlas (HPA) databases. The current research aimed to explore potential hub genes that may be highly correlated with the prognostic value of PDAC from a multicultural perspective with systems biology. An integrated analysis of the DEGs in PDAC will provide further insight into the mechanism of PDAC.

Materials and methods
PDAC dataset preprocessing

The gene expression profile data (GSE41368, GSE43795, GSE55643, and GSE41369) of PDAC were downloaded from the public GEO database by searching with the following key terms: ('microRNA' OR 'miRNA' OR 'mRNA') AND ('pancreatic ductal adenocarcinoma' OR 'PDAC'). The publication time was not limited. All included chip datasets have the same characteristics, that is, the comparison of human PDAC and normal specimens, and included at least six corresponding samples as well as all the microarray data available to the public.

Data processing

GEO2R (https://www.ncbi.nlm.nih.gov/geo/geo2r/) is an interactive online tool that can compare different groups in a GEO series and can be employed to identify DEGs and DEmiRNAs. Subsequently, by default, the adjusted *P*-values were selected to decrease the false-positive rate using the Hochberg false discovery rate and the Benjamini method. A *P*-value <0.05 and an absolute log fold-change (FC) greater than 1 for the DEGs and 2 for the DEmiRNAs were used

as the cut-off criteria. We also used the online tool Venny 2.1 (http://bioinfogp.cnb.csic.es/tools/venny/index.html) to identify the overlapping DEGs that were up-/down-regulated in the GSE41368, GSE43795, and GSE55643 datasets.

Functional enrichment analysis of the overlapping DEGs and DEmiRNAs

GO terms and KEGG (Kyoto Encyclopedia of Genes and Genomes) pathway enrichment analyses play a vital role in identifying characteristic biological attributes for high-throughput transcriptome data. We used Metascape (http://metascape.org/), a gene annotation, and analysis resource [23], to perform a functional enrichment analysis, which included cellular component (CC), molecular function (MF), and biological process (BP), and a KEGG pathway analysis of the overlapping DEGs. Similarly, we also performed a functional enrichment analysis of the DEmiRNAs using FunRich, which is also primarily used for the interaction network and the functional enrichment analysis of genes and proteins [24]. Bubble diagrams and bar charts, respectively, were used to visualize the results of the GO terms and KEGG pathway enrichment analyses of the overlapping DEGs and DEmiRNAs.

Construction of the PPI network of the overlapping DEGs

STRING (https://string-db.org/) is a user-friendly online system that provides predicted and experimental interactions of proteins [25]. We used the STRING database to analyze functional interactions between the overlapping DEGs with a confidence score of ≥ 0.4 for significant differences. The PPI network was visualized with Cytoscape (version 3.6.0, www.cytoscape.org), and the properties of the network topology for nodes were calculated to identify hub genes with a degree >5 in the present study. The degree indicates the number of edges connected with a specific node, and nodes with a high degree were identified as hub genes (i.e., may contribute to vital biological behaviors).

Survival analysis of the DEmiRNAs and hub genes

We used the KM plotter (http://kmplot.com/analysis/) [26] to perform an OS analysis of the DEmiRNAs and hub genes in 178 and 177 patients with PDAC, respectively. The plotter endows users with the ability to separate patients divided into high and low expression groups on the basis of the gene transcriptional expression level of a given gene and create KM plots. In addition, the hazard ratio (HR) with the 95% confidence interval and the log-rank *P*-value were calculated and are shown on the chart, and the number-at-risk is displayed below the curves.

Expression levels and correlation analysis of the hub genes

GEPIA (Gene Expression Profiling Interactive Analysis) is a well-developed interactive online server applied to a standard processing pipeline that analyzes the RNA sequencing expression data of 9736 tumors and 8587 normal samples from The Cancer Genome Atlas (TCGA) and the Genotype-Tissue Expression (GTEx) projects [27]. We used GEPIA to investigate the mRNA expression levels of hub genes in PDAC and normal tissues. Then, a boxplot was generated to show the relation. The HPA (https://www.proteinatlas.org/) is an open access to enable scientists in both industry and academia to freely access data for exploration of the human proteome [28]. The HPA database was also used to validate the immunohistochemistry of the candidate hub genes. The direct link to these images in the HPA are as follows: https://www.proteinatlas.org/ENSG00000136997-MYC/tissue/pancreas#img (v-myc avian myelocytomatosis viral oncogene homolog, MYC, in normal tissue); https://www.proteinatlas.org/ENSG00000136997-MYC/pathology/tissue/pancreatic+cancer#img (MYC in tumor tissue); https://www.proteinatlas.org/ENSG00000117394-SLC2A1/tissue/pancreas#img (solute carrier family 2 member 1, SLC2A1, in normal tissue); https://www.proteinatlas.org/ENSG00000117394-SLC2A1/pathology/tissue/pancreatic+cancer#img (SLC2A1 in tumor tissue); https://www.proteinatlas.org/ENSG00000067225-PKM/tissue/pancreas#img (Pyruvate kinase muscle isozymes, PKM, in normal tissue); https://www.proteinatlas.org/ENSG00000067225-PKM/pathology/tissue/pancreatic+cancer#img (PKM in tumor tissue); https://www.proteinatlas.org/ENSG00000122861-PLAU/tissue/pancreas#img (plasminogen activator, urokinase, PLAU, in normal tissue); https://www.proteinatlas.org/ENSG00000132170-PPARG/tissue/pancreas#img (peroxisome proliferator activated receptor (PPAR) γ, PPARG, in normal tissue); https://www.proteinatlas.org/ENSG00000132170-PPARG/pathology/tissue/pancreatic+cancer#img (PPARG in tumor tissue); https://www.proteinatlas.org/ENSG00000105976-MET/tissue/pancreas#img (MET proto-oncogene, receptor tyrosine kinase, MET, in normal tissue); https://www.proteinatlas.org/ENSG00000105976-MET/pathology/tissue/pancreatic+cancer#img (MET in tumor tissue); https://www.proteinatlas.org/ENSG00000005884-ITGA3/tissue/pancreas#img (integrin subunit α 3, ITGA3, in normal tissue); and https://www.proteinatlas.org/ENSG00000005884-ITGA3/pathology/tissue/pancreatic+cancer#img (ITGA3 in tumor tissue). A correlation analysis presents pairwise genes using the Pearson, Spearman, and Kendall correlation statistics based on GTEx and/or TCGA expression data in GEPIA [18].

Table 1 The data characteristics of the gene expression profiling studies

PMID	Record	mRNA/miRNA	Tissue	Normal	Tumor	Platfrom	Reference
24120476	GSE41368	mRNA	PDAC	6	6	GPL6244-[HuGene-1_0-st]Affymetrix Human Gene 1.0 ST Array [transcript (gene) version]	Frampton et al., 2014
24072181	GSE43795	mRNA	PDAC	6	6	GPL10558-Illumina HumanHT-12 V4.0 expression beadchip	Kim et al., 2014
25415223	GSE55643	mRNA	PDAC	8	45	GPL6480 Agilent-014850 Whole Human Genome Microarray 4x44K G4112F (Probe Name version)	Jamieson et al., 2014
24120476	GSE41369	miRNA	PDAC	9	9	GPL16142 NanoString nCounter Human miRNA assay (v1)	Frampton et al., 2014

Construction of the miRNA–mRNA network

The genes targeted by the DEmiRNAs were predicted using miRTarBase (http://miRTarBase.mbc.nctu.edu.tw/), the experimentally validated miRNA–target interactions database [29]. Next, the regulatory network of the predicted genes and miRNAs that targeted them were visualized in Cytoscape.

Results

Identification of the DEGs and DEmiRNAs

The characteristics of the available profiles are presented and include the PubMed ID, GEO accession number, experiment type, sample source, number of tumors and controls, platforms, corresponding author, and publication time (Table 1). As shown in Table 1, 57 PDAC samples and 20 normal samples were applied for RNA-seq analysis, and 9 PDAC samples and 9 normal samples were employed for miRNA-seq analysis. For the GSE41369 dataset, a total of 32 DEmiRNAs (24 up-regulated and 8 down-regulated miRNAs, Figure 1A and Table 2) were extracted, and a total of 1828, 3233, and 1144 genes were extracted from the GSE41368, GSE43795, and GSE55643 datasets, respectively (Figure 1B–D); these miRNAs and genes were recognized as differentially expressed in PDAC samples compared with normal samples. Among them, 150 DEGs overlapped; 76 were up-regulated (Figure 1E), and 74 were down-regulated (Figure 1F). Additionally, based on the logFC value, we show the top 25 up- and down-regulated DEGs as a heat map in Figure 1G.

Enrichment analysis of the overlapping DEGs and miRNAs

The BP analysis demonstrated that the overlapping DEGs were dramatically concentrated in cellular chemical homeostasis, carboxylic acid biosynthetic process, and the positive regulation of cell migration (Figure 2A). Regarding MF, the overlapping DEGs were significantly enriched in cell adhesion molecule binding (Figure 2B). Regarding CC, the overlapping DEGs were significantly enriched in the extracellular matrix and the external side of the plasma membrane (Figure 2C). Additionally, the KEGG analysis indicated that the overlapping DEGs were significantly enriched in pathways involved in cancer and the PI3K-Akt signaling pathway (Figure 2D).

To improve our understanding of the biological information of the 32 DEmiRNAs in PDAC, we also performed GO annotation and KEGG pathway analyses. Regarding BP, the DEmiRNAs were significantly enriched in signal transduction and cell communication as well as the regulation of nucleobase, nucleoside, nucleotide, and nucleic acid metabolism (Figure 3A). Regarding MF, the DEmiRNAs were significantly enriched in transcription factor activity and GTPase activity (Figure 3B). In addition, the most enriched GO terms in CC were nucleus, cytoplasm, Golgi apparatus, and lysosome (Figure 3C). As shown in Figure 3D, the most enriched KEGG pathway terms for the DEmiRNAs were related to VEGF and the VEGFR signaling network, the glypican pathway, LKB1 signaling events, the ERBB receptor signaling network and the sphingosine 1-phosphate (S1P) pathway.

To explore the interactions of the overlapping DEGs, a PPI network based on the STRING database was constructed. In total, the PPI network of the overlapping DEGs comprises 83 nodes and 99 edges (Figure 4). The more characteristic properties of node degree, the more significant influence it has on maintaining the stability of the PPI network. Seven nodes were identified as hub genes with a degree > 5, namely, MYC (degree = 15), SLC2A1 (degree = 7), PKM (degree = 7), PLAU (degree = 7), PPARG/PPARγ (degree = 6), MET (degree = 6), and ITGA3 (degree = 6).
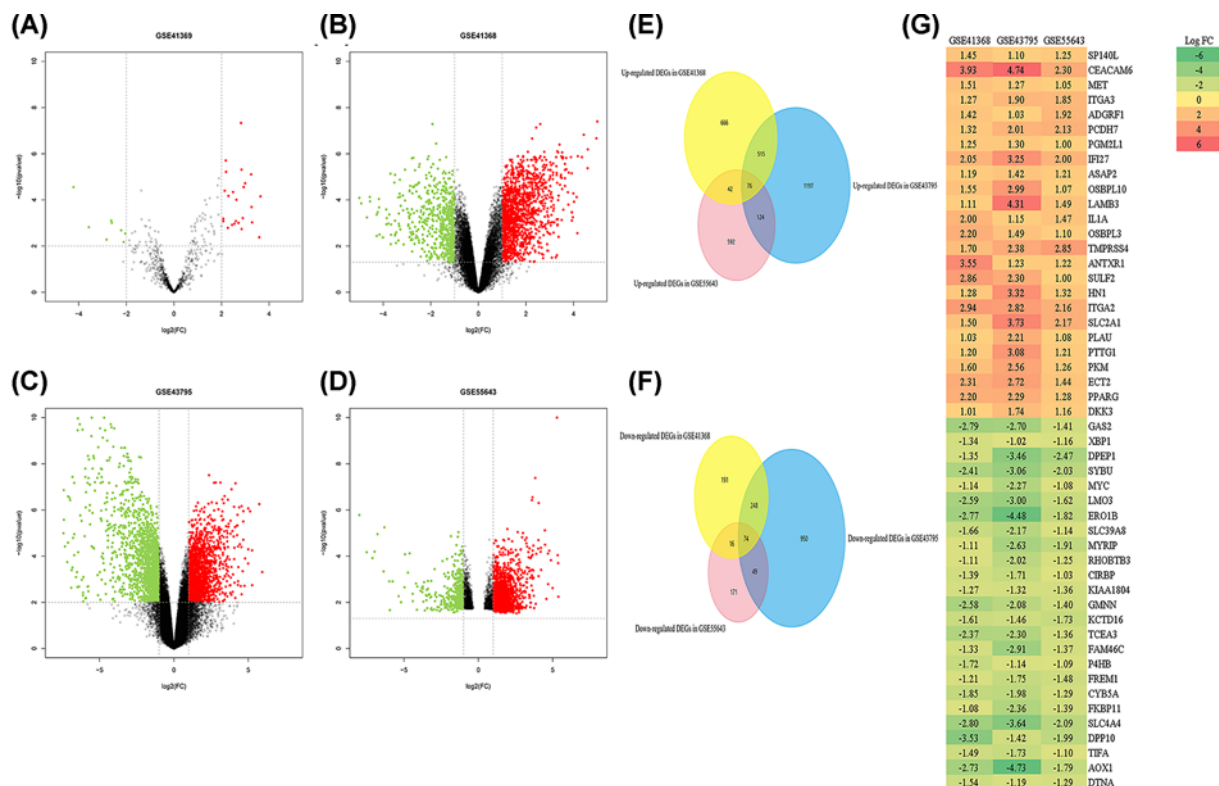
Figure 1. Volcano plot of gene expression profile data in PDAC and normal samples and the heatmap of the overlapping DEGs

(**A**) Volcano plot of GSE41369, (**B**) volcano plot of GSE41368, (**C**) volcano plot of GSE43795, (**D**) volcano plot of GSE55643, (**E**) Venn diagram of the up-regulated overlapping DEGs, (**F**) Venn diagram of the down-regulated overlapping DEGs, and (**G**) heatmap of the overlapping DEGs. Green represents a low FC value, and red represents a high FC value. Each column represents one dataset, and each row represents one gene. The number in each rectangle represents the FC in PDAC samples compared with normal samples. The gradual color change from red to green represents the changing process from up-regulation to down-regulation.

Survival analysis

KM plotter was employed to predict the prognostic values of the 32 identified DEmiRNAs and 7 hub genes. Among the DEmiRNAs examined, our results showed that the high expression of hsa-miR-221, hsa-miR-135b, hsa-miR-21, hsa-miR-199b-5p, hsa-miR-143, hsa-miR-27a, and hsa-miR-196a ($P<0.05$) was associated with worse OS for PDAC patients (Figure 5A–G). Additionally, low expression levels of hsa-miR-655, hsa-miR-455-3p, and hsa-miR-744 ($P<0.05$) were associated with poor OS for PDAC patients (Figure 5H–J). Similarly, the high expression of MYC, SLC2A1, PKM, PLAU, PPARG, MET, and ITGA3 may also be associated with the poor survival of patients with PDAC ($P<0.05$) (Figure 6).

Transcriptional expression level of the hub genes and correlation analysis

As shown in Figure 7, the mRNA expression levels of seven genes were remarkably up-regulated in PDAC based on data from the GEPIA database. In addition, we used the 'HPA' to examine the protein expression levels of these hub genes and observed that the protein expression levels of the hub genes were noticeably up-regulated in tumor tissues compared with normal tissues (Figure 8). The increase in SLC2A1, PKM, PLAU, PPARG, MET, and ITGA3 was strongly associated with the increase in MYC in PDAC (Figure 9).

miRNA–mRNA network

The network of DEmiRNAs and predicted targets is presented in Figure 10. Notably, hsa-miR-135b targeted 137 genes, including MYC; hsa-miR-221 targeted 504 genes, including PKM; hsa-miR-21 targeted 686 genes, including MYC; hsa-miR-27a targeted 467 genes, including PPARG and MET; hsa-miR-199b-5p targeted 111 genes, including ITGA3; hsa-miR-143 targeted 595 genes; hsa-miR-196a targeted 507 genes, including MYC; hsa-miR-655 targeted 224 genes,

Table 2 The up-/down-regulated DEmiRNAs in GSE41369

Up/down	DEmiRNAs	adj.P.Val	P-value	logFC
Up-regulated	hsa-miR-135b	0.0000337	4.63E-08	2.819987
	hsa-miR-221	0.0007128	1.96E-06	2.181648
	hsa-miR-10a	0.0011033	4.87E-06	2.841119
	hsa-miR-197	0.0011033	6.07E-06	2.192276
	hsa-miR-145	0.0011327	7.79E-06	3.244704
	hsa-miR-21	0.0019778	1.90E-05	2.992536
	hsa-miR-223	0.0020383	2.80E-05	2.930734
	hsa-miR-342-3p	0.0024343	4.02E-05	2.136132
	hsa-miR-125a-5p	0.002574	4.60E-05	2.483418
	hsa-miR-1975	0.0034239	6.74E-05	2.291544
	hsa-miR-27a	0.0034239	7.06E-05	3.636233
	hsa-miR-142-5p	0.0039221	9.87E-05	2.625738
	hsa-miR-199a-5p	0.0070605	2.04E-04	3.264147
	hsa-miR-142-3p	0.0159969	6.14E-04	2.892267
	hsa-miR-129-3p	0.0159969	6.56E-04	2.073776
	hsa-miR-199b-5p	0.0161787	8.32E-04	2.598735
	hsa-let-7i	0.0161787	8.37E-04	2.073183
	hsa-miR-150	0.0175298	9.44E-04	3.28386
	hsa-miR-143	0.0175298	9.89E-04	2.713456
	hsa-miR-100	0.0180691	1.08E-03	2.544108
	hsa-miR-199a/b-3p	0.0194912	1.21E-03	2.445292
	hsa-miR-23a	0.0215577	1.63E-03	2.265833
	hsa-miR-125b	0.0233466	1.83E-03	2.846407
	hsa-miR-196a	0.0413646	4.15E-03	3.586379
Down-regulated	hsa-miR-630	0.0020383	2.80E-05	−4.218462
	hsa-miR-216a	0.0161787	7.81E-04	−2.636217
	hsa-miR-130b	0.0175298	9.84E-04	−2.612345
	hsa-miR-217	0.0211921	1.52E-03	−3.572319
	hsa-miR-655	0.0260153	2.08E-03	−2.216555
	hsa-miR-455-3p	0.0301557	2.86E-03	−2.038336
	hsa-miR-744	0.0492626	5.24E-03	−2.830606
	hsa-miR-220a	0.0542844	6.66E-03	−2.109385

Table 3 The interactive relationship between hub genes and miRNAs

Hub genes	DEmiRNAs
MYC	hsa-miR-196a, hsa-miR-21, hsa-miR-135b, hsa-miR-744, hsa-miR-455-3p, hsa-miR-655
SLC2A1	NA
PKM	hsa-miR-221
PLAU	NA
PPARG	hsa-miR-27a
MET	hsa-miR-27a
ITGA3	hsa-miR-199b-5p

The intersection of DEGs in the miRNAs–mRNA regulatory network
P4HB, RUNX2, MYC, BNIP3, PKM, PGM2L1, BTG2, SERPINB5, ACAT1, COBLL1, JADE1, SERPINI1, LIFR, OSBPL3, CXCL10, FGF12, ECT2, MET PPARG, OSBPL10, CYB5A, LAMC2, ITGA3, HK2, ABAT, REEP3, PHGDH, ITGA2, PTTG1, LIPH, SLC25A15.

including MYC; hsa-miR-455-3p targeted 784 genes, including MYC; and hsa-miR-744 targeted 665 genes, including MYC. As a group, a total of 31 of the 150 DEGs were contained in the miRNA–mRNA regulatory network (Figure 10 and Table 3).
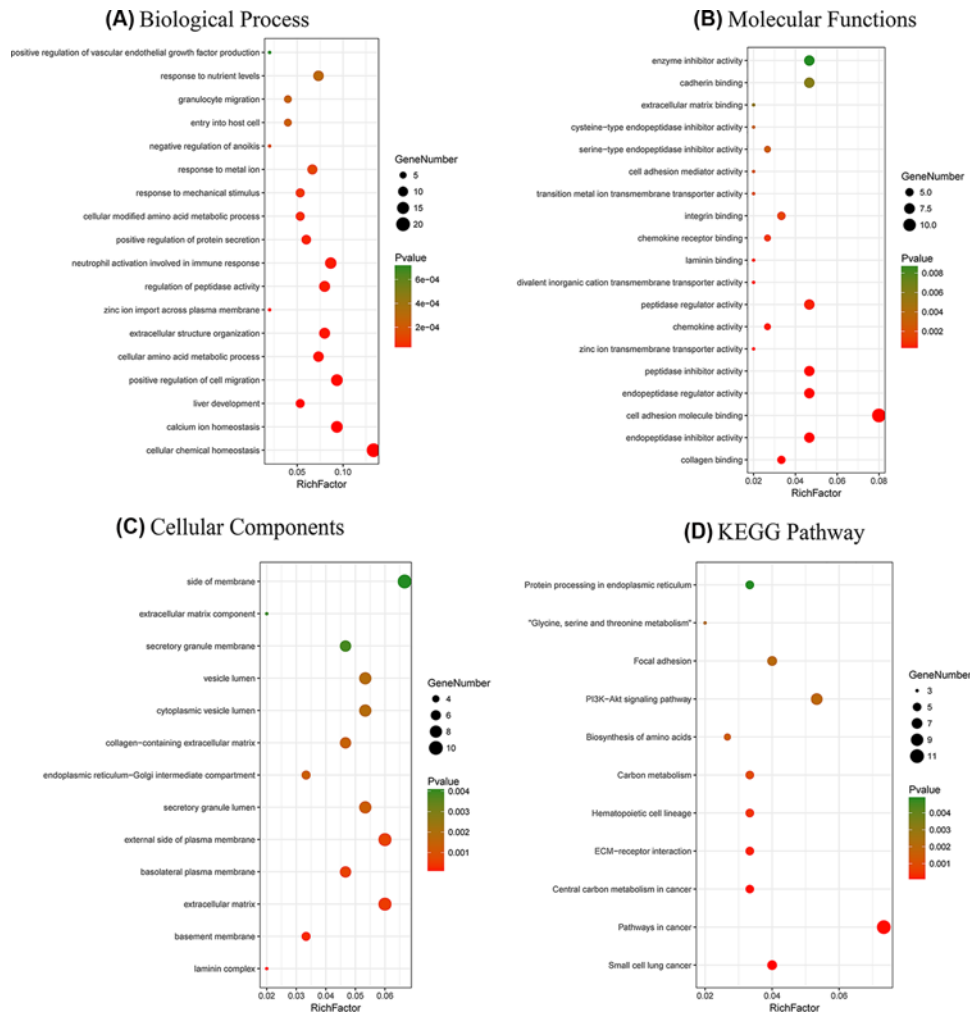
Figure 2. Functional and pathway enrichment analyses of the overlapping DEGs in PDAC

(**A**) BP, (**B**) MF, (**C**) CC, (**D**) and KEGG pathway analyses. The x-axis represents the q value (−log10), and the y-axis represents the GO term. The GO terms were measured by the rich factor, q value and number of genes enriched. The greater the Rich factor is, the greater the degree of enrichment and the greater the p value [0, 1]. The brighter the color of red is, the more significant the term.

Discussion

MiRNAs can be used as biological markers for PCs [4,30], and PC is becoming a common malignant disease with an incidence that has continued to rise during the last few years [30,31]. Hence, specific biomarkers for accurate diagnostic tests and potential therapeutic targets for individualized therapy are yet to be fully determined in PDAC. In the current study, the mRNA and miRNA expression data obtained from the GEO database yielded an overall total of 150 genes (76 up-regulated and 74 down-regulated genes) and 32 miRNAs (24 up-regulated and 8 down-regulated miRNAs) that were differentially expressed in PDAC samples and normal tissues. The 150 DEGs were significantly enriched in cancer-related pathways. Moreover, 32 DEmiRNAs were significantly enriched in the glypican pathway. The glypicans comprise a family of glycosylphosphatidylinositol (GPI)-anchored heparan sulfate proteoglycans that has a remarkable effect on cell division and growth regulation. At present, six members (GPC1–6) of this family are recognized in vertebrates [32]. The glypican pathway, which was indicated in the KEGG pathway analysis, includes glypican 1 (GPC1, Entry: k08107), which promotes the pathogenesis of many human cancers [33]. Research shows that high levels of serum GPC1 indicate a poor prognosis in PDAC [34], suggesting that intervention of the glypican pathway may be a promising strategy for PDAC treatment. The increased expression of seven DEmiRNAs (miR-135b, miR-221, miR-21, miR-27a, miR-199b-5p, miR-143, and miR-196a) and seven hub genes (MYC, SLC2A1, PKM, PLAU, PPARG, MET, and ITGA3) were associated with worse OS; however, hsa-miR-655, hsa-miR-455-3p, and
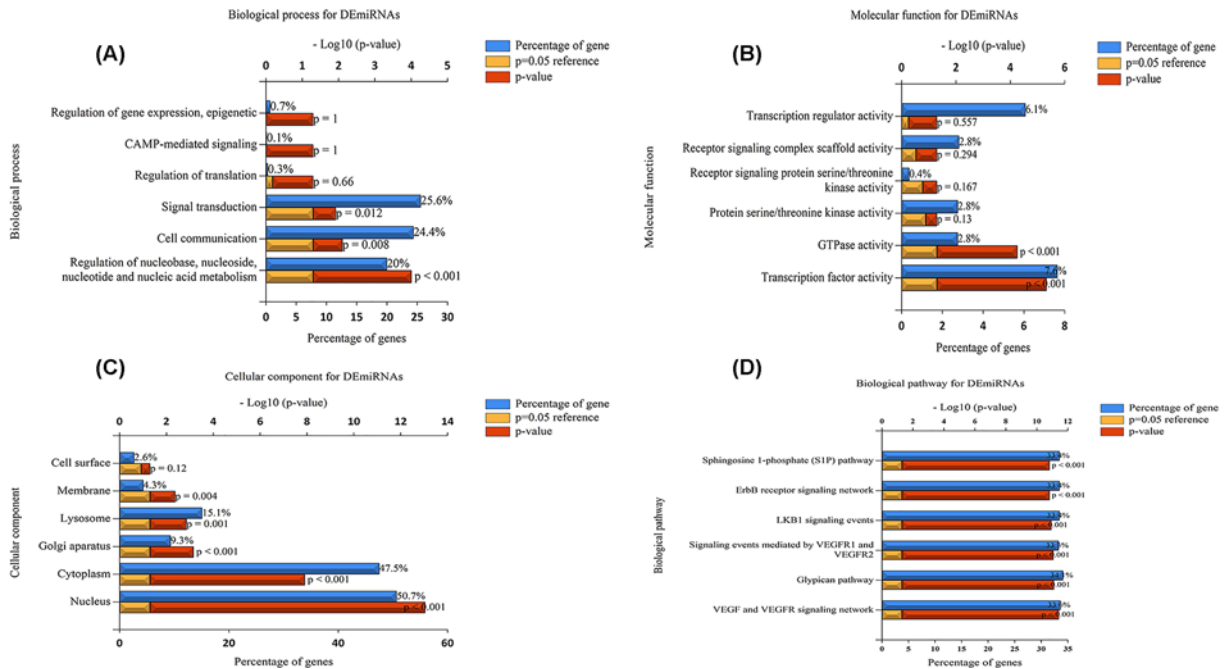
Figure 3. Functional and pathway enrichment analyses of the DEmiRNAs in PDAC
(**A**) The BP analysis of miRNAs related to the DEGs, (**B**) the MF analysis of the miRNAs related to the DEGs, (**C**) the CC analysis of the miRNAs related to the DEGs, (**D**) and the biological pathway analysis of the miRNAs related to the DEGs. The upper x-axis represents the *P*-value (−log10), and the lower x-axis represents the percentage of genes (blue). The y-axis represents the GO term. Yellow represents the *P*-value equal to 0.05 as reference, and red represents the specific *P*-value. The longer the rectangular zone, the smaller the *P*-value is.

hsa-miR-744 had the opposite prognostic value. SLC2A1, PKM, PLAU, PPARG, MET, and ITGA3 were up-regulated in PDAC compared with normal tissues and were closely related to an increase in MYC.

MiRNAs can function as competing endogenous RNAs (ceRNAs), causing the degradation and/or inhibition of mRNA translation by binding to its 3′−untranslated region (3′-UTR) [35]. However, this function is not exactly consistent with the aforementioned pattern between the DEmiRNAs and hub genes, which may also play a prominent role in tumor onset and progression in PDAC. Munding et al. (2012) [36] showed that miR-135b was highly misregulated and was preferable to miR-196a and miR-210 as an indicator for identifying PDAC. Similarly, Han et al. (2017) [37] reported that miR-135b-5p was significantly up-regulated in PC tissue compared with adjacent tissue, and the overexpression of miR-135b-5p advanced proliferation and migration by decreasing the transcriptional expression level of SFRP4 by directly targeting its 3′-UTR. Wang et al. (2016) [38] showed that miR-221 bound to the 3′-UTR of endothelial nitric oxide synthase traffic inducer (NOSTRIN) and inhibited its expression, and up-regulated miR-221 expression correlated with unsatisfactory survival in PDAC, and another study demonstrated that miR-221 is an oncogenic miRNA that contributes to Capan-2 cell proliferation by regulating the PTEN-Akt pathway [39]. In addition, miR-21 promotes epidermal growth factor (EGF)-induced proliferation, inhibits cell apoptosis, and accelerates cell cycle progression by targeting the PI3K/AKT and MAPK/ERK signaling pathways [40]; it is also associated with poor OS and disease-free survival in PDAC [41]. Frampton et al. (2015) [42] identified three miRNAs (miR-21, miR-23a, and miR-27a) with high tumor expression, and the inhibition of miR-23a, miR-21, and miR-27a had promoting effects in decreasing the proliferation of PDAC cells in culture and the growth of xenograft tumors. A fibrotic tumor-associated stroma (TAS), which is believed to aggravate the clinical biological symptoms of PDAC, and miR-199a and miR-199b, which belong to the miR-199 family that is uniquely expressed in TAS cells, support the stromal miRNA feature, suggesting that the tumor microenvironment contributes to miRNA changes, which conversely have mechanical effects on the TAS [43]. Compared with normal tissues, miR-143 was up-regulated in both PDAC and PVAC tumor samples, which may reflect the histological features and biological behavior of different PCs [44]. Accumulating evidence indicates that the serum miR-196a expression level is able to predict the median survival time of PDAC patients [45,46]. The OS analysis of the up-regulated DEmiRNAs was consistent with the results
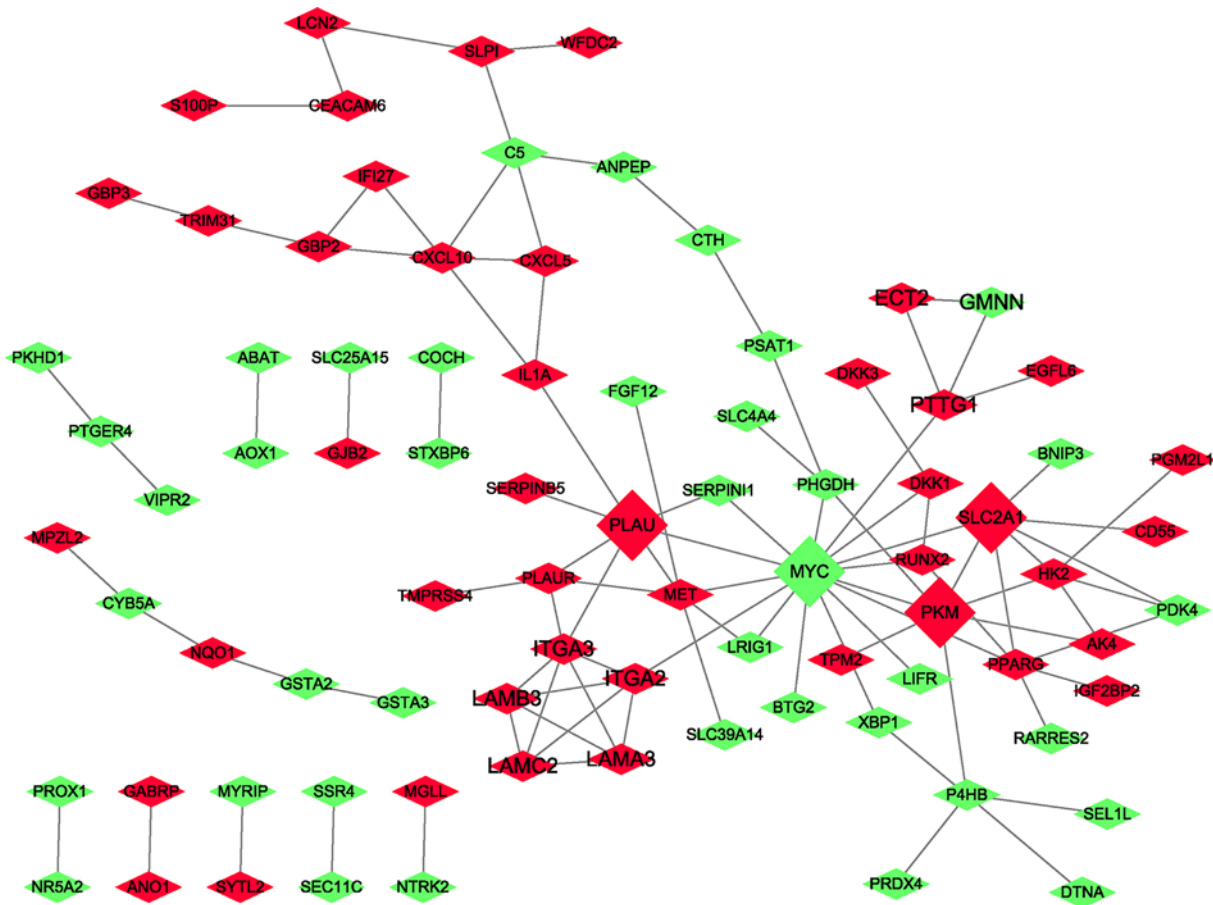
Figure 4. PPI network analysis of the overlapping DEGs
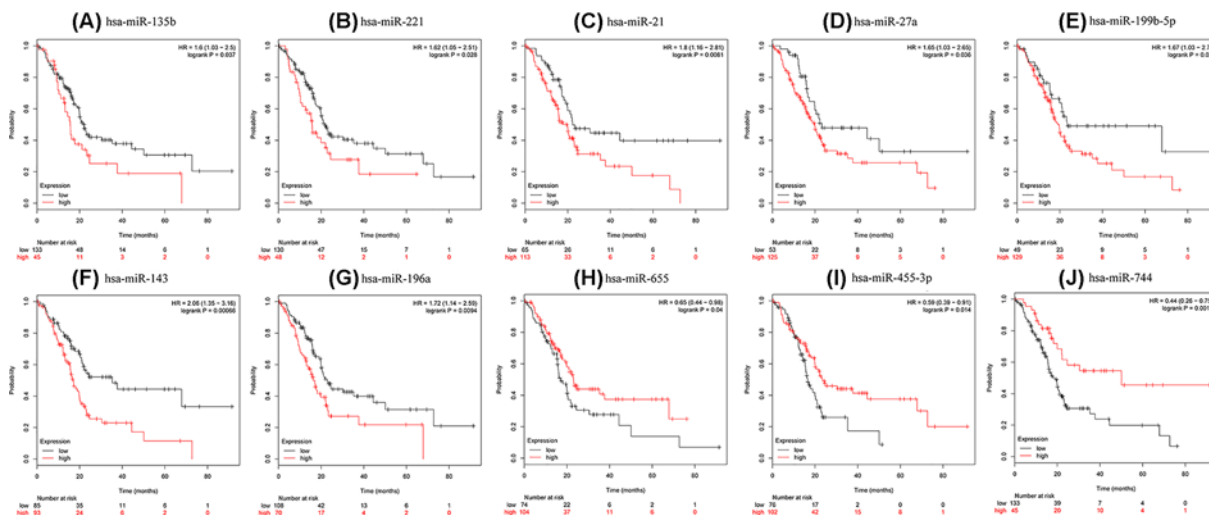Red nodes, up-regulated genes; green nodes, down-regulated genes.

Figure 5. Overall survival analyses of differentially expressed microRNAs
KM curves depicting OS for PDAC patients with high and low expression of (**A**) hsa-miR-135b, (**B**) hsa-miR-221, (**C**) hsa-miR-21, (**D**) hsa-miR-27a, (**E**) hsa-miR-199b-5p, (**F**) hsa-miR-143, (**G**) hsa-miR-196a, (**H**) hsa-miR-655, (**I**) hsa-miR-455-3p, and (**J**) hsa-miR-744.
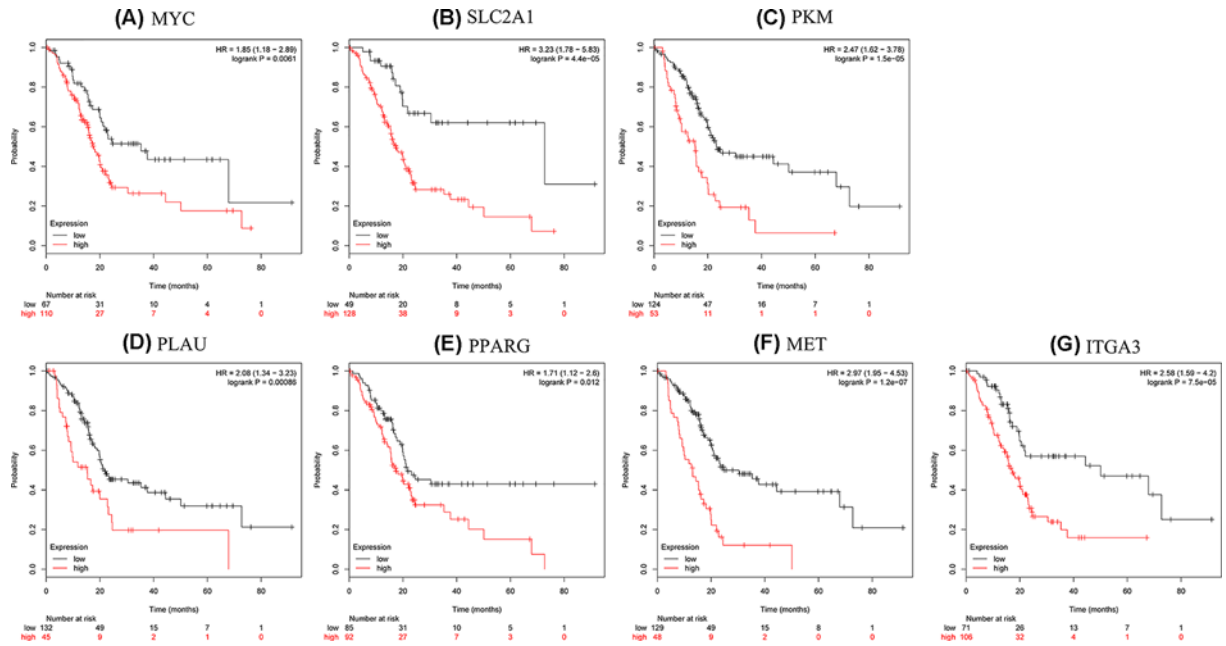
Figure 6. Prognostic value of seven DEGs in PC patients

Prognostic value of (**A**) MYC (log-rank P-value = 0.0061), (**B**) SLC2A1 (log-rank P-value = 4.4e-05), (**C**) PKM (log-rank P-value = 1.5e-05), (**D**) PLAU (log-rank P-value = 0.00086), (**E**) PPARG (log-rank P-value = 0.012), (**F**) MET (log-rank P-value = 1.2e-07), and (**G**) ITGA3 (log-rank P-value = 7.5e-05).
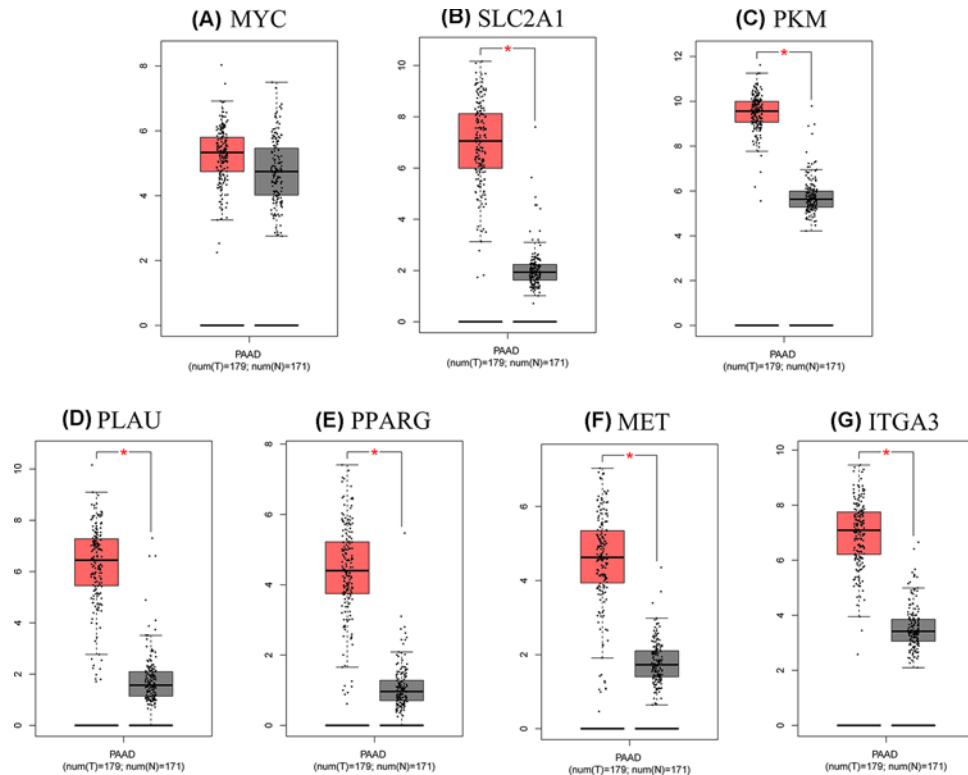

Figure 7. Expression levels of seven hub genes in human pancreatic adenocarcinoma

(**A**) MYC; (**B**) SLC2A1; (**C**) PKM; (**D**) PLAU; (**E**) PPARG; (**F**) MET; and (**G**) ITGA3. The gray and red boxes represent normal and cancer tissues, respectively. The expression data are first log2(TPM+1) transformed for differential analysis and the log2FC is defined as median (Tumor, T)-median(Normal, N). *$P<0.05$, T vs N. Abbreviations: FC, fold change; TPM, transcript per kilobase million.
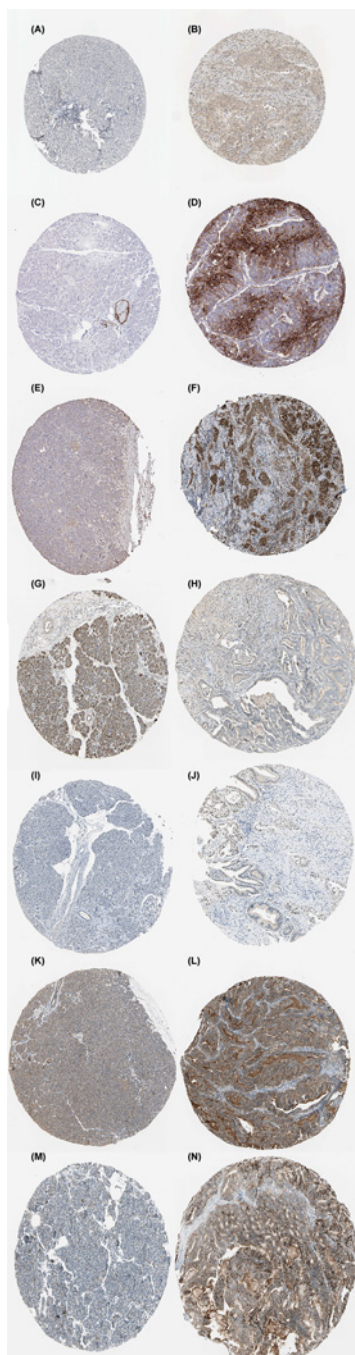
Figure 8. Immunohistochemistry of the five hub genes based on the HPA

(**A**) Protein levels of MYC in normal tissue (staining: low; intensity: weak; quantity: >75%). (**B**) Protein levels of MYC in tumor tissue (staining: medium; intensity: moderate; quantity: 75–25%). (**C**) Protein levels of SLC2A1 in normal tissue (staining: not detected; intensity: negative; quantity: negative). (**D**) Protein levels of SLC2A1 in tumor tissue (staining: high; intensity: strong; quantity: 75–25%). (**E**) Protein levels of PKM in normal tissue (staining: low; intensity: weak; quantity: 75–25%). (**F**) Protein levels of PKM in tumor tissue (staining: high; intensity: strong; quantity: >75%). (**G**) Protein levels of PLAU in normal tissue (staining: not detected; intensity: negative; quantity: negative). (**H**) Protein levels of PLAU in tumor tissue (staining: low; intensity: weak; quantity: >75%). (**I**) Protein levels of PPARG in normal tissue (staining: not detected; intensity: negative; quantity: negative). (**J**) Protein levels of PPARG in tumor tissue (staining: medium; intensity: moderate; quantity: 75–25%). (**K**) Protein levels of MET in normal tissue (staining: medium; intensity: moderate; quantity: >75%). (**L**) Protein levels of MET in tumor tissue (staining: medium; intensity: moderate; quantity: >75%). (**M**) Protein levels of ITGA3 in normal tissue (staining: low; intensity: weak; quantity: >75%). (**N**) Protein levels of ITGA3 in tumor tissue (staining: high; intensity: strong; quantity: >75%).
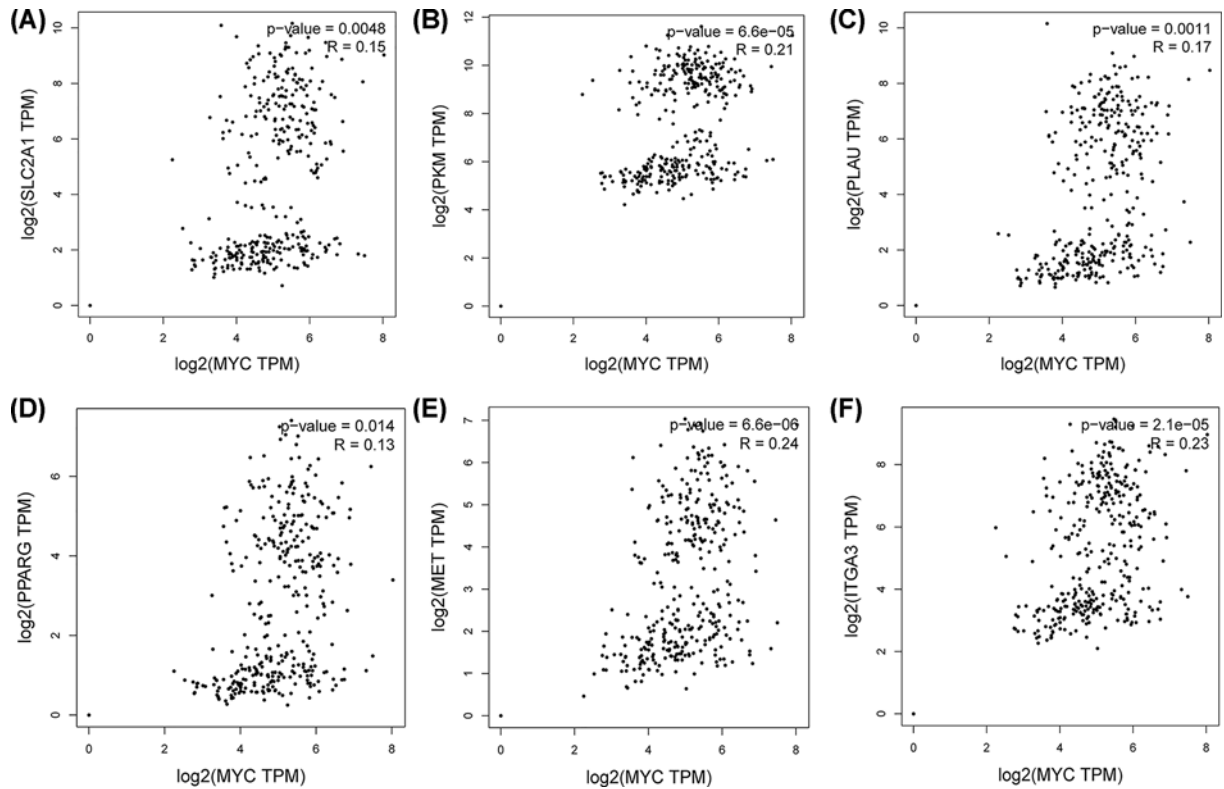
Figure 9. Correlation analysis of SLC2A1, PKM, PLAU, PPARG, MET, ITGA3, and MYC in pancreatic adenocarcinoma
(**A**) SLC2A1, (**B**) PKM, (**C**) PLAU, (**D**) PPARG, (**E**) MET, and (**F**) ITGA3. TPM, transcript per million. The x-axis represents the TPM of the hub gene, MYC (log2), the y-axis represents the TPM of the hub genes SLC2A1, PKM, PLAU, PPARG, MET, and ITGA3 (log2). The expression levels of SLC2A1, PKM, PLAU, PPARG, MET, and ITGA3 were positively correlated with the MYC expression level.

of the present study. Epithelial-to-mesenchymal transition (EMT) has been reported to promote cancer progression. Harazono et al. (2013) [47] reported that the overexpression of miR-655, which is an EMT-suppressive miRNA that targets TGFBR2 and ZEB1, not only induced the up-regulation of E-cadherin and the downregulation of typical EMT inducers but also inhibited the invasion and migration of mesenchymal-like cancer cells. Furthermore, the upregulation of miR-655 inhibits cell invasion in esophageal squamous cell carcinoma [48], triple-negative breast cancer [49], and hepatocellular carcinoma [50]. MiRNA-455 (miR-455) is recognized as a broadly conserved noncoding RNA that has been implicated in various cancers. The function of miR-455 has been confirmed in prostate cancer [51], gastric cancer [52], and oral squamous cancer cells [53]. However, the potential effect of miR-455-3p has rarely been explored in PDAC. In the current study, the survival analysis demonstrated that the up-regulated expression of miR-455-3p in PDAC patients was associated with prolonged OS. miR-744 was found to be significantly up-regulated in PC and increased tumorigenicity by inhibiting multiple negative regulators of the Wnt/β-catenin pathway [54]. Furthermore, a high level of plasma miR-744 contributed to the poor progression-free survival of nonoperable PC patients [55]. Interestingly, contradictory results regarding the survival analysis in this study demonstrate that further investigation is needed to confirm the effect of miR-744.

MYC acts as a carcinogenic transcription factor that regulates at least 15% of genes involved in various cellular processes, including the differentiation, cell proliferation, apoptosis, and metabolism of PC [56,57]. Additionally, the KRAS/ERK/c-Myc axis is the major driving factor of tumorigenesis in PC. In normal cells, MYC is a transient protein that is present from 20 to 30 min and is uncontrollable in cancers. Hence, promoting the degradation of MYC is a promising treatment strategy for PDAC [57]. Metabolic deregulation is a hallmark of human cancers. SLC2A1, also named GLUT1, transports glucose and its analogs into cells. A previous study indicated that the up-regulation of SLC2A1 accelerated tumor cell proliferation and metastasis [58]. Pyruvate kinase muscle isozymes (PKMs) play an important role in adjusting metabolic changes during carcinogenesis. Cheng et al. (2018) [59] revealed that the increased expression of PKM1 and PKM2 affected cell invasion and migration in PDAC cells. Lu et al. (2018) [60] analyzed the related microarray datasets (GSE15471, GSE62452, GSE102238, GSE62165, and GSE16515) and identified
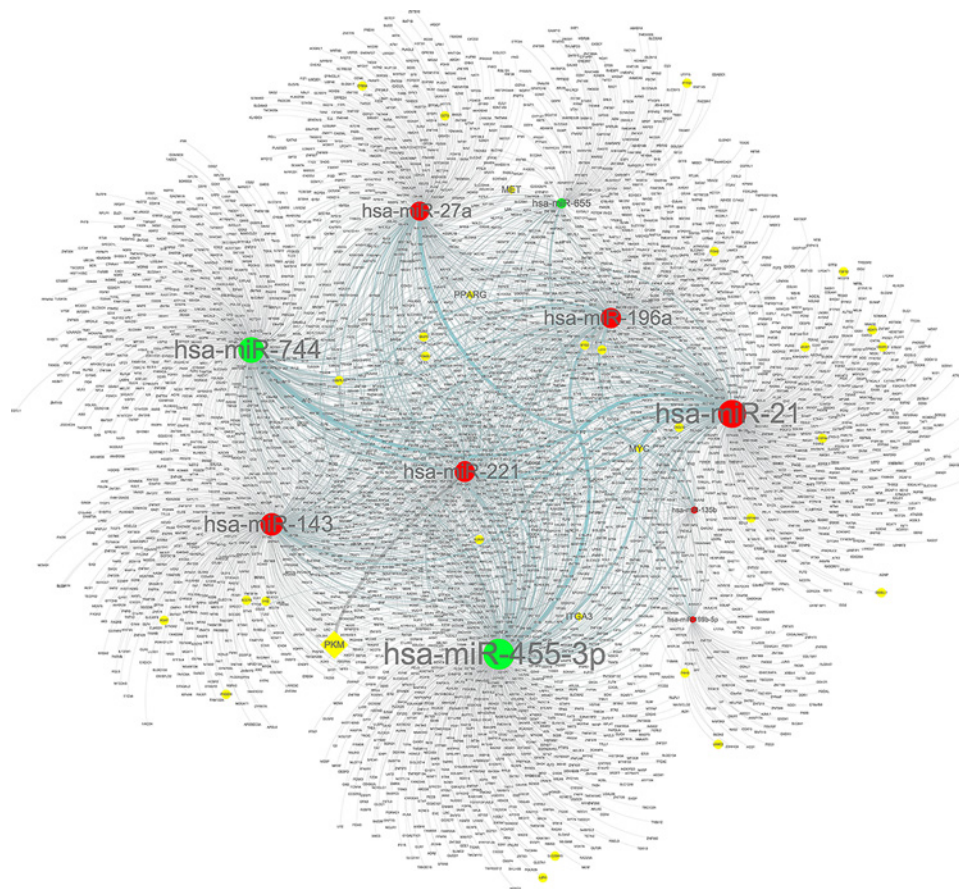
Figure 10. Regulatory network of the predicted genes and their target miRNAs
Circle nodes indicate DEmiRNAs. Diamond nodes represent hub genes. Red nodes represent up-regulated DEmiRNAs, and green nodes represent down-regulated DEmiRNAs. Yellow nodes indicate DEGs.

the top 21 genes with high connectivity degrees; among them, PLAU is a plasminogen activator, ITGA3 plays a vital function in EMT, and the high expression of PLAU and ITGA3 is related to poor survival, consistent with the current research. The peroxisome proliferator activated receptors (PPARs), a member of the NR1 (thyroid-like) subfamily of NR, comprise PPARα (NR1C1), PPARβ/δ (NR1C2), and PPARγ (NR1C3). PPARγ, which is expressed in primary PDAC and has proven to be of clinical value when used as an independent prognostic factor, is closely related to a high clinical stage and has a close association with short OS [61]. MET, the receptor of hepatocyte growth factor, was identified as a cancer stem cell marker in PDAC. Tomihara et al. (2017) [62] also revealed that patients with high Met expression experienced a markedly shorter survival time than those with low Met expression, consistent with the current research. Altogether, these data support that the DEmiRNAs and hub genes shed light on the clinical utility of prognostic values in PDAC.

The combination of a multichip joint analysis and a bioinformatics analysis has a notable advantage in recognizing and confirming possible biomarkers and targets for malignant tumors, although there are some limitations to the current study. First, the number of samples in each microarray dataset was relatively small, which may have resulted in a few false-positive results, and second, these results were not validated; therefore, further mechanistic studies of larger samples are still needed in the future.

Taken together, the results of the bioinformatics analysis of four GEO microarray datasets of PC indicated that cancer-related pathways (KEGG Entry: k05200) and the glypican pathway (KEGG Entry: k08107) probably participate in the onset and development of PDAC. The high expression of miR-135b, miR-221, miR-21, miR-27a, miR-199b-5p, miR-143, miR-196a, MYC, SLC2A1, PKM, PLAU, PPARG, and ITGA3, as well as the low expression of miR-655, miR-455-3p, and miR-744, were observably related to unsatisfactory survival effects in patients with PDAC. Bioinformatics analyses revealed that different miRNAs exhibited diverse potential functions that were associated with the DEGs. However, further studies need to be implemented to explore the molecular mechanisms

and biological functions of the miRNA/target gene axis and to estimate whether they can serve as novel potential biomarkers or therapeutic targets in PC patients.

Author Contribution

J.Z. and L.F. conceived and designed the study. J.Z. and X.H. wrote the manuscript. J.Z. and Y.M. analyzed and interpreted the data. All authors read and approved the final manuscript.

Competing Interests

The authors declare that there are no competing interests associated with the manuscript.

Funding

Abbreviations

ANXA2 , annexin A2; BP , biological process; CC, cellular component; DEG, differentially expressed gene; DEmiRNA, differentially expressed microRNA; EMT, epithelial-to-mesenchymal transition; FC, fold-change; GEO, Gene Expression Omnibus; GEPIA , Gene Expression Profiling Interactive Analysis; GPC1 , glypican 1; GTEx, Genotype-Tissue Expression; HPA, Human Protein Atlas; ITGA3, integrin subunit α 3; KEGG , Kyoto Encyclopedia of Genes and Genomes; KM , Kaplan–Meier; MET, MET proto-oncogene, receptor tyrosine kinase; MF, molecular function; miRNA , microRNA; mRNA, messenger RNA; MYC , V-myc avian myelocytomatosis viral oncogene homolog; OS, overall survival; PC, pancreatic cancer; PDAC, pancreatic ductal adenocarcinoma; PLAU, plasminogen activator, urokinase; PPARG, peroxisome proliferator activated receptor γ; PPI, protein–protein interaction; SLC2A1, solute carrier family 2 member 1; TAS, tumor-associated stroma; TCGA, The Cancer Genome Atlas.

References

1 Zhao, X., Ren, Y., Cui, N., Wang, X. and Cui, Y. (2018) Identification of key microRNAs and their targets in exosomes of pancreatic cancer using bioinformatics analysis. *Medicine* **97**, e12632, https://doi.org/10.1097/MD.0000000000012632

2 Zhang, Z., Pan, B., Lv, S. et al. (2018) Integrating microRNA expression profiling studies to systematically evaluate the diagnostic value of MicroRNAs in pancreatic cancer and validate their prognostic significance with the cancer genome atlas data. *Cell. Physiol. Biochem.* **49**, 678–695, https://doi.org/10.1159/000493033

3 Shi, G., Zhang, J., Lu, Z. et al. (2017) A novel messenger RNA signature as a prognostic biomarker for predicting relapse in pancreatic ductal adenocarcinoma. *Oncotarget* **8**, 110849–110860, https://doi.org/10.18632/oncotarget.22861

4 Kojima, M., Sudo, H. and Kawauchi, J. (2015) MicroRNA markers for the diagnosis of pancreatic and biliary-tract cancers. *PLoS ONE* **10**, e0118220, https://doi.org/10.1371/journal.pone.0118220

5 Yan, W. and Yan, L. (2015) Analysis of molecular pathways in pancreatic ductal adenocarcinomas with a bioinformatics approach. *Asian Pac. J. Cancer Prev.* **16**, 2561–2567, https://doi.org/10.7314/APJCP.2015.16.6.2561

6 Shen, Q., Yu, M. and Jia, J.K. (2018) Possible molecular markers for the diagnosis of pancreatic ductal adenocarcinoma. *Med. Sci. Monit.* **24**, 2368–2376, https://doi.org/10.12659/MSM.906313

7 Khan, S. (2015) Cancer and the microbiome: potential applications as new tumor biomarker. *Expert Rev. Anticancer Ther.* **15**, 317–330, https://doi.org/10.1586/14737140.2015.992785

8 Arthur, J.C., Perez-Chanona, E., Muhlbauer, M. et al. (2012) Intestinal inflammation targetscancer-inducing activity of the microbiota. *Science* **338**, 120–123, https://doi.org/10.1126/science.1224820

9 Khan, S. et al. (2017) Prediction of mycoplasma hominis proteins targeting in mitochondria and cytoplasm of host cells and their implication in prostate cancer etiology. *Oncotarget* **8**, 30830–30843, https://doi.org/10.18632/oncotarget.8306

10 Zakariah, M. et al. (2018) To decipher the mycoplasma hominis proteins targeting into the endoplasmic reticulum and their implications in prostate cancer etiology using next-generation sequencing data. *Molecules* **23**, 994, https://doi.org/10.3390/molecules23050994

11 Khan, S., Imran, A. and Khan, A.A. (2016) Systems Biology approaches for the prediction of possible role of *Chlamydia pneumoniae* proteins in the etiology of lung cancer. *PLoS ONE* **11**, e0148530, https://doi.org/10.1371/journal.pone.0148530

12 Shahanavaj, K. (2015) Potential role of *Escherichia coli* DNA mismatch repair proteins in colon cancer. *Crit. Rev. Oncol. Hematol.* **96**, 475–482, https://doi.org/10.1016/j.critrevonc.2015.05.002

13 Su, Q., Zhu, E.C., Qu, Y.L. et al. (2018) Serum level of co-expressed hub miRNAs as diagnostic and prognostic biomarkers for pancreatic ductal adenocarcinoma. *J Cancer* **9**, 3991–3999, https://doi.org/10.7150/jca.27697

14 Lv, F., Zheng, K., Yu, J. et al. (2018) MicroRNA-661 expression is upregulated in pancreatic ductal adenocarcinoma and promotes cell proliferation. *Oncol. Lett.* **16**, 6293–6298

15 Wei, D.M., Dang, Y.W., Feng, Z.B. et al. (2018) Biological effect and mechanism of the miR-23b-3p/ANXA2 axis in pancreatic ductal adenocarcinoma. *Cell. Physiol. Biochem.* **50**, 823–840, https://doi.org/10.1159/000494468

16 Alshamsana, A.W.S. (2017) Prediction of *Chlamydia pneumoniae* protein localization in host mitochondria and cytoplasm and possible involvements in lung cancer etiology: a computational approach. *Saudi Pharm. J.* **25**, 1151–1157, https://doi.org/10.1016/j.jsps.2017.05.007

17 Khan, S. et al. (2016) Computational prediction of *Mycoplasma hominis* proteins targeting in nucleus of host cell and their implication in prostate cancer etiology. *Tumour Biol.* **37**, 10805–10813, https://doi.org/10.1007/s13277-016-4970-9

18 Yi, H.C., Liu, Y.L., You, P., Pan, J.S., Zhou, J.Y., Liu, Z.J. et al. (2015) Overexpression of DEK gene is correlated with poor prognosis in hepatocellular carcinoma. *Mol. Med. Rep.* **11**, 1318, https://doi.org/10.3892/mmr.2014.2781

19 Barrett, T., Wilhite, S.E., Ledoux, P., Evangelista, C., Kim, I.F., Tomashevsky, M. et al. (2013) NCBI GEO: archive for functional genomics data sets-update. *Nucleic Acids Res.* **41**, D991–D995, https://doi.org/10.1093/nar/gks1193

20 Frampton, A.E., Castellano, L., Colombo, T., Giovannetti, E. et al. (2014) MicroRNAs cooperatively inhibit a network of tumor suppressor genes to promote pancreatic tumor growth and progression. *Gastroenterology* **146**, 268.e18–277.e18, https://doi.org/10.1053/j.gastro.2013.10.010

21 Park, M., Kim, M., Hwang, D., Park, M. et al. (2014) Characterization of gene expression and activated signaling pathways in solid-pseudopapillary neoplasm of pancreas. *Mod. Pathol.* **27**, 580–593, https://doi.org/10.1038/modpathol.2013.154

22 Lunardi, S., Jamieson, N.B., Lim, S.Y., Griffiths, K.L. et al. (2014) IP-10/CXCL10 induction in human pancreatic cancer stroma influences lymphocytes recruitment and correlates with poor survival. *Oncotarget* **5**, 11064–11080, https://doi.org/10.18632/oncotarget.2519

23 Tripathi, S., Pohl, M.O., Zhou, Y., Rodriguez-Frandsen, A., Wang, G., Stein, D.A. et al. (2015) Meta-and orthogonal integration of influenza "OMICs" data defines a role for UBR4 in virus budding. *Cell Host Microbe* **18**, 723–735, https://doi.org/10.1016/j.chom.2015.11.002

24 Pathan, M., Keerthikumar, S., Chisanga, D. et al. (2017) A novel community driven software for functional enrichment analysis of extracellular. *J. Extracell. Vesicles* **6**, 1321455, https://doi.org/10.1080/20013078.2017.1321455

25 Shen, S., Kong, J., Qiu, Y. et al. (2019) Identification of core genes and outcomes in hepatocellular carcinoma by bioinformatics analysis. *J. Cell. Biochem.* **120**, 10069–10081, https://doi.org/10.1002/jcb.28290

26 Lanczky, A., Nagy, A., Bottai, G., Munkacsy, G., Paladini, L., Szabo, A. et al. (2016) miRpower: a web-tool to validate survival-associated miRNAs utilizing expression data from 2,178 breast cancer patients. *Breast Cancer Res. Treat.* **160**, 439–446, https://doi.org/10.1007/s10549-016-4013-7

27 Tang, Z., Li, C. and Kang, B. (2017) GEPIA: a web server for cancer and normal gene expression profiling and interactive analyses. *Nucleic Acids Res.* **45**, W98–W102, https://doi.org/10.1093/nar/gkx247

28 Uhlén, M., Fagerberg, L., Hallström, B.M. et al. (2015) Proteomics. Tissue-based map of the human proteome. *Science* **347**, 1260419, https://doi.org/10.1126/science.1260419

29 Chou, C.H., Shrestha, S. and Yang, C.D. (2018) miRTarBase update 2018: a resource for experimentally validated microRNA-target interactions. *Nucleic Acids Res.* **46**, D296–D302, https://doi.org/10.1093/nar/gkx1067

30 Liu, B., Yang, H. and Taher, L. (2018) Identification of prognostic biomarkers by combined mRNA and miRNA expression microarray analysis in pancreatic cancer. *Transl. Oncol.* **11**, 700–714, https://doi.org/10.1016/j.tranon.2018.03.003

31 Malvezzi, M., Carioli, G., Bertuccio, P., Boffetta, P., Levi, F., La Vecchia, C. et al. (2017) European cancer mortality predictions for the year 2017, with focus on lung cancer. *Ann. Oncol.* **28**, 1117–1123, https://doi.org/10.1093/annonc/mdx033

32 Szpirer, C., Szpirer, J., Riviere, M., Van Vooren, P., Veugelers, M. and David, G. (2001) Mapping of the rat glypican genes. *Cytogenet. Cell Genet.* **93**, 83–86, https://doi.org/10.1159/000056954

33 Li, J., Chen, Y., Zhan, C. et al. (2019) Glypican-1 promotes tumorigenesis by regulating the PTEN/Akt/β-catenin signaling pathway in esophageal squamous cell carcinoma. *Dig Dis. Sci.* **64**, 1493–1502, https://doi.org/10.1007/s10620-019-5461-9

34 Zhou, C.-Y., Dong, Y.-P., Sun, X. et al. (2018) High levels of serum glypican-1 indicate poor prognosis in pancreatic ductal adenocarcinoma. *Cancer Med.* **7**, 5525–5533, https://doi.org/10.1002/cam4.1833

35 Liang, L., Wei, D.-M., Li, J.-J. et al. (2017) Prognostic microRNAs and their potential molecular mechanism in pancreatic cancer: a study based on The Cancer Genome Atlas and bioinformatics investigation. *Mol. Med. Rep.* **17**, 939–951

36 Munding, J.B., Adai, A.T. and Maghnouj, A. (2012) Global microRNA expression profiling of microdissected tissues identifies miR-135b as a novel biomarker for pancreatic ductal adenocarcinoma. *Int. J. Cancer* **131**, E86–E95, https://doi.org/10.1002/ijc.26466

37 Han, X., Saiyin, H. and Zhao, J. (2017) Overexpression of miR-135b-5p promotes unfavorable clinical characteristics and poor prognosis via the repression of SFRP4 in pancreatic cancer. *Oncotarget* **8**, 62195–62207

38 Wang, J., Yang, S. and He, P. (2016) Endothelial nitric oxide synthase traffic inducer (NOSTRIN) is a negative regulator of disease aggressiveness in pancreatic cancer. *Clin. Cancer Res.* **22**, 5992–6001, https://doi.org/10.1158/1078-0432.CCR-16-0511

39 Yang, W., Yang, Y., Xia, L. et al. (2016) MiR-221 promotes Capan-2 pancreatic ductal adenocarcinoma cells proliferation by targeting PTEN-Akt. *Cell. Physiol. Biochem.* **38**, 2366–2374, https://doi.org/10.1159/000445589

40 Zhang, L., Yao, J., Li, W. et al. (2017) Micro-RNA-21 regulates cancer-associated fibroblast-mediated frug resistance in pancreatic cancer. *Oncol. Res.* **26**, 827–836, https://doi.org/10.3727/096504017X14934840662335

41 Guraya, S. (2018) Prognostic significance of circulating microRNA-21 expression in esophageal, pancreatic and colorectal cancers; a systematic review and meta-analysis. *Int. J. Surg.* **60**, 41–47, https://doi.org/10.1016/j.ijsu.2018.10.030

42 Frampton, A.E., Castellano, L. and Colombo, T. (2015) Integrated molecular analysis to investigate the role of microRNAs in pancreatic tumour growth and progression. *Lancet* **385**, S37, https://doi.org/10.1016/S0140-6736(15)60352-X

43 Han, S., Gonzalo, D.H., Feely, M. et al. (2017) The pancreatic tumor microenvironment drives changes in miRNA expression that promote cytokine production and inhibit migration by the tumor associated stroma. *Oncotarget* **8**, 54054–54067

44 Tavano, F., Mola, F.F.D. and Piepoli, A. (2012) Changes in miR-143 and miR-21 expression and clinicopathological correlations in pancreatic cancers. *Pancreas* **41**, 1280–1284, https://doi.org/10.1097/MPA.0b013e31824c11f4

45 Xu, Y.F., Hannafon, B.N. and Zhao, Y.D. (2017) Plasma exosome miR-196a and miR-1246 are potential indicators of localized pancreatic cancer. *Oncotarget* **8**, 77028–77040

46 Yu, Q., Xu, C., Yuan, W. et al. (2017) Evaluation of plasma microRNAs as diagnostic and prognostic biomarkers in pancreatic adenocarcinoma: miR-196a and miR-210 could be negative and positive prognostic markers, respectively. *Biomed. Res. Int.* **2017**, 6495867, https://doi.org/10.1155/2017/6495867

47 Harazono, Y., Muramatsu, T. and Endo, H. (2013) miR-655 Is an EMT-suppressive microRNA targeting ZEB1 and TGFBR2. *PLoS ONE* **8**, e62757, https://doi.org/10.1371/journal.pone.0062757

48 Wang, Y., Zang, W. and Du, Y. (2013) Mir-655 up-regulation suppresses cell invasion by targeting pituitary tumor-transforming gene-1 in esophageal squamous cell carcinoma. *J. Transl. Med.* **11**, 301, https://doi.org/10.1186/1479-5876-11-301

49 Lv, Z.-D., Kong, B., Liu, X.-P. et al. (2016) MiR-655 suppresses epithelial-to-mesenchymal transition by targeting Prrx1 in triple-negative breast cancer. *J. Cell. Mol. Med.* **20**, 864–873, https://doi.org/10.1111/jcmm.12770

50 Wu, G., Zheng, K. and Xia, S. (2016) MicroRNA-655-3p functions as a tumor suppressor by regulating ADAM10 and β-catenin pathway in hepatocellular carcinoma. *J. Exp. Clin. Cancer Res.* **35**, 1–12

51 Zhao, Y., Yan, M., Yun, Y. et al. (2017) MicroRNA-455-3p functions as a tumor suppressor by targeting eIF4E in prostate cancer. *Oncol. Rep.* **37**, 2449–2458, https://doi.org/10.3892/or.2017.5502

52 Liu, J., Zhang, J. and Li, Y. (2016) MiR-455-5p acts as a novel tumor suppressor in gastric cancer by down-regulating RAB18. *Gene* **592**, 308–315, https://doi.org/10.1016/j.gene.2016.07.034

53 Cheng, C.M., Shiah, S.G., Huang, C.C., Hsiao, J.R. and Chang, J.Y. (2016) Upregulationof miR-455-5p by the TGF-b-SMAD signalling axis promotes the proliferation of oral squamous cancer cells by targeting UBE2B. *J. Pathol.* **240**, 38–49, https://doi.org/10.1002/path.4752

54 Zhou, W., Li, Y. and Gou, S. (2015) MiR-744 increases tumorigenicity of pancreatic cancer by activating Wnt/β-catenin pathway. *Oncotarget* **6**, 37557–37569, https://doi.org/10.18632/oncotarget.5317

55 Mahito, M., Shuhei, K. and Daisuke, I. (2015) Plasma microRNA profiles: identification of miR-744 as a novel diagnostic and prognostic biomarker in pancreatic cancer. *Br. J. Cancer* **113**, 1467–1476, https://doi.org/10.1038/bjc.2015.366

56 Hessmann, E., Schneider, G. and Ellenrieder, V. (2015) MYC in pancreatic cancer: novel mechanistic insights and their translation into therapeutic strategies. *Oncogene* **35**, 1609–1618, https://doi.org/10.1038/onc.2015.216

57 Wirth, M., Mahboobi, S., Kramer, O.H. and Schneider, G. (2016) Concepts to target MYC in pancreatic cancer. *Mol. Cancer Ther.* **15**, 1792–1798, https://doi.org/10.1158/1535-7163.MCT-16-0050

58 Yan, S., Wang, Y., Chen, M., Li, G. and Fan, J. (2015) Deregulated SLC2A1 promotes tumor cell proliferation and metastasis in gastric cancer. *Int. J. Mol. Sci.* **16**, 16144–16157, https://doi.org/10.3390/ijms160716144

59 Cheng, T.Y., Yang, Y.C. and Wang, H.P. (2018) Pyruvate kinase M2 promotes pancreatic ductal adenocarcinoma invasion and metastasis through phosphorylation and stabilization of PAK2 protein. *Oncogene* **37**, 1730–1742, https://doi.org/10.1038/s41388-017-0086-y

60 Lu, Y., Li, C., Chen, H. and Zhong, W. (2018) Identification of hub genes and analysis of prognostic values in pancreatic ductal adenocarcinoma by integrated bioinformatics methods. *Mol. Biol. Rep.* **45**, 1799–1807, https://doi.org/10.1007/s11033-018-4325-2

61 Polvani, S., Tarocchi, M. and Tempesti, S. (2014) Nuclear receptors and pathogenesis of pancreatic cancer. *World J. Gastroenterol.* **20**, 12062–12081, https://doi.org/10.3748/wjg.v20.i34.12062

62 Tomihara, H., Yamada, D. and Eguchi, H. (2017) MiR-181b-5p, ETS1 and c-Met pathway exacerbates the prognosis of pancreatic ductal adenocarcinoma after radiation therapy. *Cancer Sci.* **108**, 398–407, https://doi.org/10.1111/cas.13159